THE JOURNAL OF PHYSICAL CHEMISTRY C

Article

pubs.acs.org/JPCC

Observation of Low-Frequency Combination and Overtone Raman Modes in Misoriented Graphene

Juanxia Wu,[†,‡] Hua Xu,[†] Weihua Mu,[§,∥,*] Liming Xie,[⊥] Xi Ling,[#] Jing Kong,[#] Mildred S. Dresselhaus,[#] and Jin Zhang[†,*]

[†]Center for Nanochemistry, Beijing National Laboratory for Molecular Sciences, Key Laboratory for the Physics and Chemistry of Nanodevices, College of Chemistry and Molecular Engineering, Peking University, Beijing 100871, China

[‡]Academy for Advanced Interdisciplinary Studies, Peking University, Beijing 100871, China

[§]State Key Laboratory of Theoretical Physics, Institute of Theoretical Physics; Kavli Institute for Theoretical Physics China, The Chinese Academy of Sciences, P.O. Box 2735, Beijing 100190, China

[∥]Department of Chemistry, Massachusetts Institute of Technology, Cambridge, Massachusetts 02139, United States

[⊥]Key Laboratory of Standardization and Measurement for Nanotechnology of Chinese Academy of Sciences, National Center for Nanoscience and Technology, Beijing 100190, China

[#]Department of Electrical Engineering and Computer Science, Massachusetts Institute of Technology, Cambridge, Massachusetts 02139, United States

Supporting Information

ABSTRACT: Stacking disorder will significantly modify the optical properties and interlayer coupling stretch of few-layer graphene. Here, we report the observation of the Raman breathing modes in the low-frequency range of 100−200 cm^{-1} in misoriented few-layer graphene on a SiO_2/Si substrate. Two dominant Raman modes are identified. The one at ∼120 cm^{-1} is assigned as the E_g + ZO′ combination mode of the in-plane shear and the out-of-plane interlayer optical phonon breathing modes. Another peak at ∼182 cm^{-1} is identified as the overtone mode 2ZO′. The appearance of these Raman modes for different twist angles indicates that stacking disorder in few-layer graphene significantly alters the Raman feature, especially for those combination modes containing the interlayer breathing mode. Further investigation shows that the two Raman vibrational modes (∼120 and ∼182 cm^{-1}) are strongly coupled to the excitation laser energy, but their frequencies are independent of the number of graphene layers before folding. The present work provides a sensitive way to study the phonon dispersion, electron−phonon interaction, and electronic band structure of misoriented graphene layers.

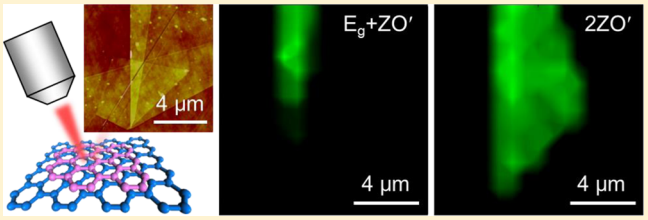

INTRODUCTION

Graphene has an ideal two-dimensional (2D) structure with a monolayer of carbon atoms arranged on a honeycomb crystal plane.[1−4] The novel physical properties of graphene arise from its unique electronic structure, in which the conduction and valence bands touch each other at two points (the K and K′ points) in the Brillouin zone.[5,6] In the vicinity of these points, the charge carriers behave like massless Dirac fermions.

The unit cell of monolayer graphene contains two inequivalent carbon atoms. In AB stacked bilayer graphene (BLG), a carbon atom of the top layer is located right over the center of the hexagon of the bottom layer. A moiré pattern is formed for a twisted bilayer graphene when the two layers are stacked with a lattice mismatch.[7,8] In twisted bilayer graphene (tBLG), the electronic band structure around the K point can be represented by two Dirac cones separated from each other by an angle corresponding to the twist angle.[9−11] Theoretical study suggested that the linear electron dispersion relationship is maintained at the K point in the tBLG with twist angle above 10°, similar to that in single-layer graphene, and van Hove singularities are generated due to the interlayer interaction.[3,7,8,12,13] Electronic flat bands at the K point can be generated when the twist angle is smaller than 1.5°.[3]

Raman spectroscopy provides a nondestructive and sensitive tool to investigate the electronic band structure, the phonon energy dispersion, and the electron−phonon interaction in carbon nanotubes and graphene systems.[14−18] It is well-known that the G′ band located at ∼2670 cm^{-1} can be fitted by four Lorentzian peaks for the AB stacked bilayer graphene, and the line shape and intensity of the G′ band can be used to estimate the number of layers.[17,19,20] For the misoriented bilayer graphene samples, the G band intensity shows a strong resonance at the critical twist angle, and the peak frequency and width show nearly no angle dependence.[10] However, the G′ band behaves as a single Lorentzian peak, similar to the single layer graphene, only at the large twist angles.[21,22] Furthermore,

Received: November 25, 2013
Revised: January 24, 2014
Published: January 28, 2014

dx.doi.org/10.1021/jp411573c | J. Phys. Chem. C 2014, 118, 3636−3643

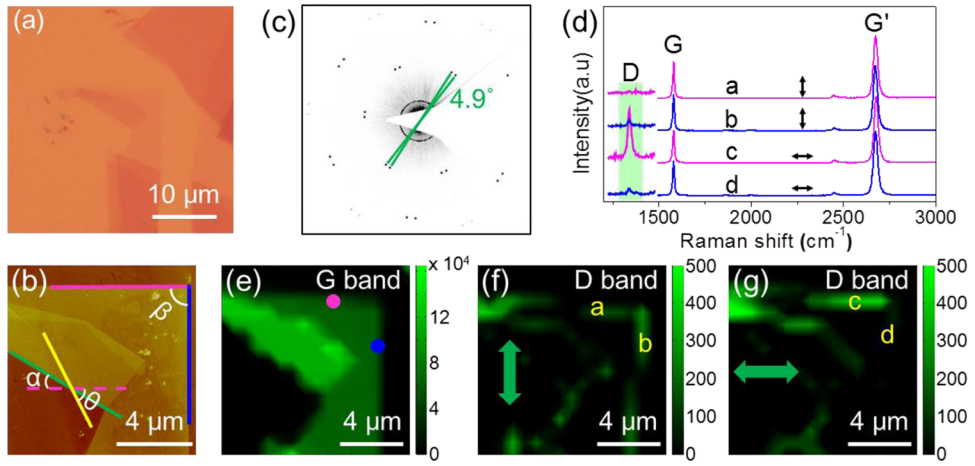

Figure 1. Determination of the twist angle and edge chirality. (a) Optical and (b) AFM images for a single-layer graphene sheet with a folded region. The angle between the two edges of the graphene sheet is labeled by $\beta = 90.4°$ with a pink and blue line in (b). (c) Diffraction pattern of the graphene sample taken in the folded region. (d) Raman spectra taken on the edges corresponding to the labels in (e–g), where spectra a and b are taken with vertical laser polarization and spectra c and d are taken with horizontal laser polarization. (e) Raman image of the G-band intensity. (f, g) Raman images of the D-band intensity with the (f) vertical and (g) horizontal laser polarizations, respectively. The excitation laser wavelength is 514.5 nm.

the G′ band intensity and line width were reported showing obvious twist angle dependence.[9,10,23] In particular, a series of extra peaks, in the range of 1000–1620 cm^{-1}, can be observed in the tBLG when the wavevector of the phonon is equal to the reciprocal lattice vectors of the moiré pattern due to the intravalley and intervalley umklapp double-resonance scattering process involving the transverse optical (TO), longitudinal optical (LO), and longitudinal acoustic (LA) phonon branches.[24,25] In addition, detailed studies have been carried out on the second-order combination modes in single-walled carbon nanotubes[26,27] and monolayer graphene.[28] Typically, it is not very easy to assign the high-frequency phonon combination modes in graphene. However, Mafra et al. assigned the phonon combination modes in the frequency range of 1700–2300 cm^{-1} in monolayer graphene using gate-modulated Raman scattering together with varying the laser excitation energy and with careful analysis of the electron–phonon interaction.[29] For high-frequency combination modes, one has to select the correct pair of phonon modes from many candidates.[28,30–32]

Besides the D, G, and G′ bands observed in single-layer graphene, the shear mode and the interlayer breathing mode (ILBM), which are rigid-plane Raman modes in few layer graphene located at 31 and 94 cm^{-1}, are also sensitive to and provide information on the layer number and stacking order of such materials.[33,34] They involve the relative motions of individual graphene layer either parallel or perpendicular to the layer plane and directly related to the van der Waals (vdW) interaction between the graphene layers. The shear mode has been measured in graphite and multilayer graphene,[33] and the ILBMs have been studied in multiwalled carbon nanotubes, graphite, as well as in few-layer and scrolled graphene.[30,32,34–38] Although many theoretical studies have focused on the low-energy shear modes and ILBMs of 2D layered materials, such as graphene and hexagonal boron nitride (h-BN),[39–43] the combination modes involving these phonon modes have not yet been comprehensively investigated in few-layer graphene.

In this paper, we have systematically studied the low-frequency combination and overtone modes in the range of 100–200 cm^{-1} for few-layer graphene with different numbers of layers and different stacking orders, and we identified these two types of Raman modes based on double-resonance theory. The E_g + ZO′ combination mode of the shear mode and ILBM and the overtone mode 2ZO′ occur around 120 and 180 cm^{-1}, respectively. For a given laser excitation energy, these two types of Raman modes can only be detected for some special twist angle values, where the restriction on the twist angle comes from the need to satisfy the momentum conservation in the double-resonance process. These special Raman modes are absent for other angles. To further understand the origin of these special Raman modes, we investigated the excitation wavelength dependence of these combination and overtone Raman modes. The results suggested that the intensities of these two Raman modes are heavily influenced by the incident laser energy. The stacking disorder between the two graphene layers will result in the form of the moiré pattern, and the reciprocal lattice vector (**G**) of the moiré superlattice can only equal to some discrete values. The momentum conservation has to be satisfied in the double-resonance Raman scattering process, which demands that the phonon scattering will be allowed only for those phonons with wave vectors **G**. Moreover, both vibrational modes are determined by interlayer interaction; thus, the presented results provide a wealth of information on the interlayer interaction of twisted bilayer graphene, much more than the studies on shear mode and ILBM of FLG separately.

■ EXPERIMENTAL SECTION

Graphene samples were prepared by the micromechanical cleavage of Kish graphite (Covalent Materials Corp.) using Scotch tape and transferred to a SiO_2/Si (300 nm thick oxide) substrate. The few-layer graphene was distinguished by both optical microscopy (OM) and Raman spectroscopy. Some graphene sheets were occasionally found to be folded after exfoliation. Raman spectra were collected on both a JY Horiba HR800 Raman system with 632.8, 514.5, and 457.9 nm laser lines and a WITEC RSA300+ Raman system with the 532 nm laser line. The gratings for both of the Raman systems had 600 lines/mm, and the spectral resolutions were about 1 and 4 cm^{-1}, respectively. A 100× objective with a numerical aperture

dx.doi.org/10.1021/jp411573c | J. Phys. Chem. C 2014, 118, 3636–3643

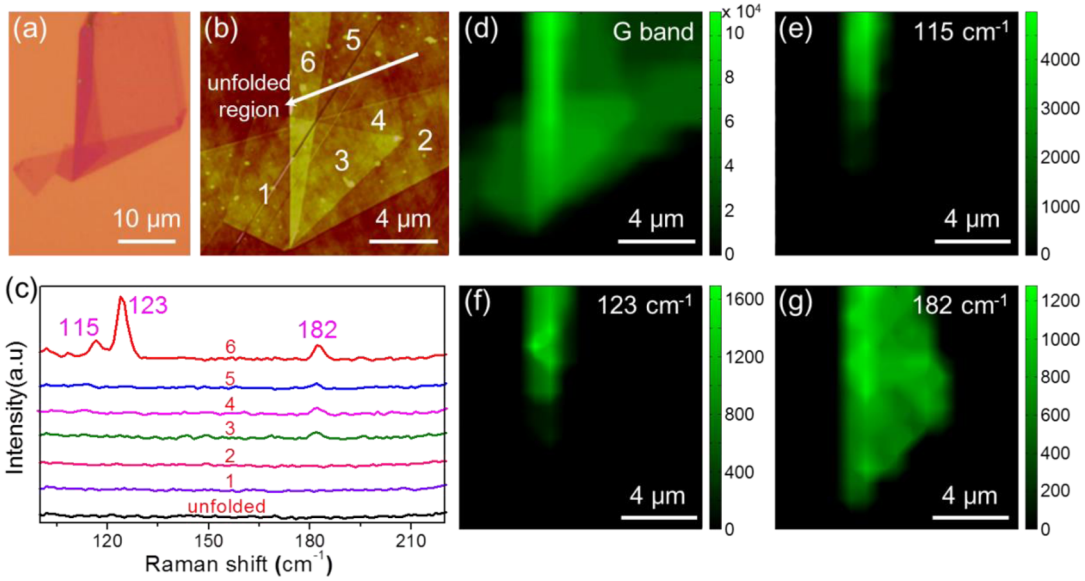

Figure 2. (a) Optical and (b) AFM images of a graphene sheet with six folded regions, labeled with 1−6 in (b). The unfolded region is the rest of the pieces of this graphene sample. (c) Raman spectra of the graphene sheet in the six folded and unfolded regions in the frequency range of 100−220 cm^{-1}. The labels on the spectra correspond to those in (b). (d−g) Mapping images of the Raman intensity of the graphene sample for (d) the G band, peak intensities at (e) 115, (f) 123, and (g) 182 cm^{-1}. The excitation laser wavelength is 632.8 nm in (c−g).

NA = 0.95 was used to focus the incident laser beam. The diameter of the laser spot was about 1 μm, and the power on the samples was kept below 0.5 mW to avoid laser-induced heating. An XYZ microscope stage with micrometer resolution was used to move the sample during the Raman mapping experiment. The intensity and Raman shift of the peaks were determined by fitting them with a Lorentzian function. The peak position was calibrated by the 520 cm^{-1} peak from the silicon substrate. Transmission electron microscopy (TEM) characterization of the misoriented graphene was carried out through transferring the exfoliated graphene sample with a folded region onto a Si_3N_4 TEM grid with an array of holes of 2 μm in diameter. The twist angle was determined by the diffraction pattern.

RESULTS AND DISCUSSION

1. Edge Chirality and Twist Angle Determinations. The moiré patterns in high-resolution STM images,[7] DF-TEM images,[9] and diffraction patterns[10] were often used to determinate the twist angle between adjacent graphene layers. The crystal orientation (either zigzag or armchair directions) of a graphene sheet can also be determined from its smooth edge. Therefore, the twist angle between adjacent layers could be obtained from their relative geometry.[21,22,44] Figure 1a,b shows the optical and AFM images of a single layer graphene with a folded region. The pink and green lines in Figure 1b indicate the crystal axis of the bottom layer of this graphene sample and of the folded edge, respectively. The yellow line in Figure 1b indicates the crystal orientation of the top layer, so that the twist angle θ can be calculated using the following relationship: $\theta = 2\alpha$ ($2\alpha < 90°$) or $\theta = 180° - 2\alpha$ ($2\alpha > 90°$).[44] It is worth pointing out that the twist angle is confined to of the range 0−30°, if the obtained angle is larger than 30°. For example, $\theta' = 60° - \theta$ for $30° < \theta < 60°$, while $\theta' = \theta - 60°$ if $\theta > 60°$. For the graphene layer in Figure 1b, $\alpha = 32.2°$, so the twist angle is ~4.4°. Figure 1c shows the diffraction pattern of the graphene sample taken from the folded region, showing two sets of the hexagonal diffraction spots, which are rotated by 4.9° with respect to one another. Good agreement between the two experimental results demonstrates the validity of the method to estimate the twist angle using an AFM image. The Raman spectra recorded in the folded and unfolded regions under 514.5 and 632.8 nm laser excitation are shown in the Supporting Information (Figure S1). The G′ band exhibits a single Lorentzian feature in the folded region, and it is blue-shifted relative to that recorded in the unfolded region, illustrating the misoriented stacking nature between the two graphene layers in the folded region.[45,46] A peak at ~1620 cm^{-1} (LO phonon mode near the Γ point) appears in the folded region, which is consistent with the fact that it is only active at a low twist angle ($3° < \theta < 8°$).[11,47] The twist angles of other folded graphene samples were obtained using a similar method.

According to double-resonance theory, a symmetry-breaking defect will be necessary for the appearance of the D band in graphene.[48] The D band that appears at the armchair edge will be much stronger than that at the zigzag edge for the ideal edges in graphene because the double-resonance process will be satisfied at the armchair edge, while this process will be symmetry forbidden for the zigzag edge (D band is a intervalley scattering process).[49−52] Raman spectra collected from the edges under different laser polarizations are shown in Figure 1d. All the spectra are collected under the same conditions and are normalized with the G band intensity. With vertical and horizontal laser polarization, spectra a and c in Figure 1d are recorded at the edge labeled with a pink circle in Figure 1e, and spectra b and d are collected from the edge labeled with the blue circle. The D band intensity is much stronger for spectrum c than for spectra a, b, and d. Since these difference are not only due to the polarization effect, but also to the edge chirality effect, we can now point out that the majority of carbon atoms along the edge marked with the blue circle in Figure 1e are arranged with zigzag chirality and another edge arranged with an armchair chirality that will show a strong D band when located parallel to the laser polarization. The Raman images of the G and D band are shown in Figure 1e−g. The G band signal is distributed homogeneously over the whole unfolded

dx.doi.org/10.1021/jp411573c | J. Phys. Chem. C 2014, 118, 3636−3643

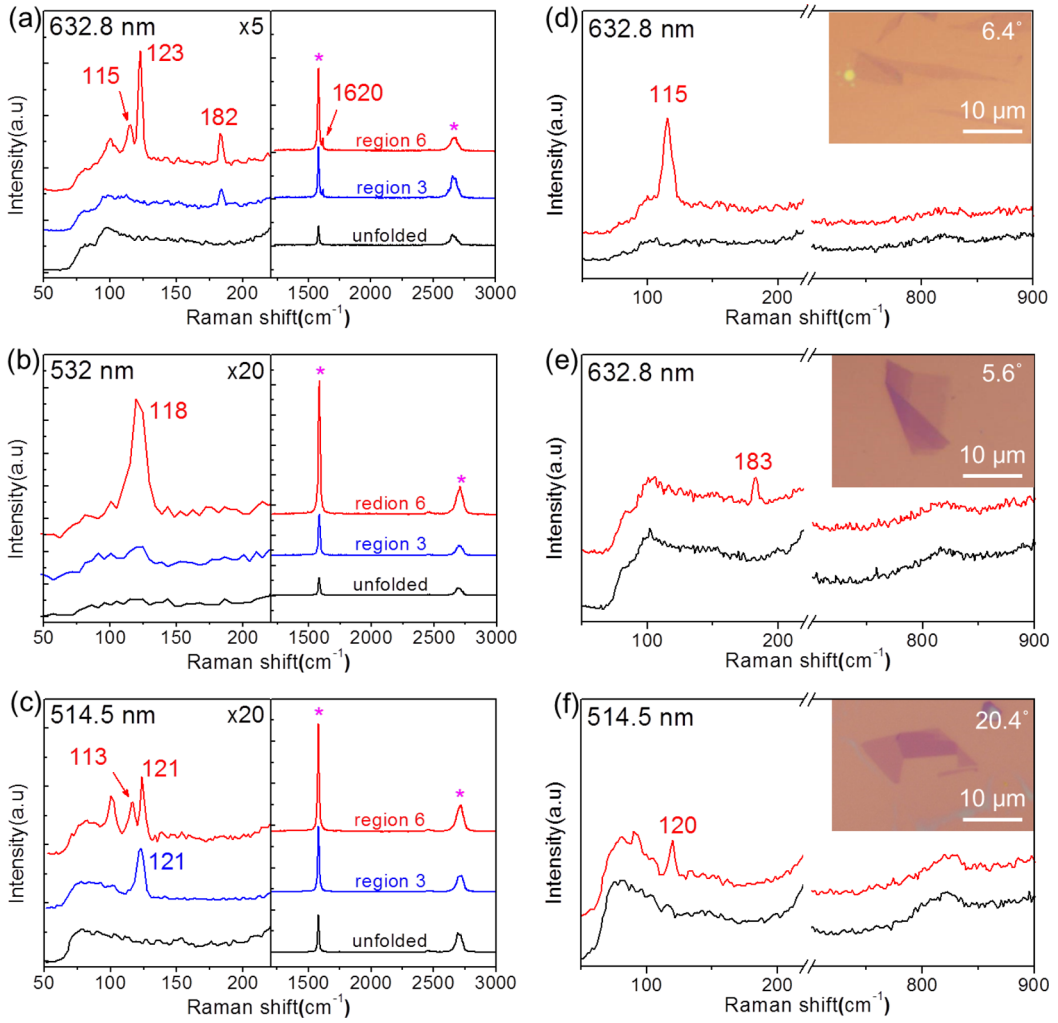

Figure 3. (a–c) Laser excitation energy and (d–f) layer number dependence of the combination and overtone Raman modes. (a–c) Raman spectra for the sample in Figure 2 under the (a) 632.8, (b) 532, and (c) 514.5 nm laser excitation energy. The spectra in red, blue, and black are corresponding to the region 6, 3, and the unfolded region, respectively. The Raman signals marked by an asterisk are the G and G′ bands of graphene. For clarity, the intensity of the spectra in the range of 50–250 cm^{-1} is magnified by a factor labeled on the upper right corner. (d–f) Raman spectra collected in the folded (red line) and unfolded (black line) regions for other graphene sheets. The frequency of the combination or overtone Raman modes are labeled. The insets show the OM images of the graphene sheets with a twist region. The twist angles are marked on the OM images. The laser excitation wavelength is 632.8 nm for (d–e) and 514.5 nm for (f).

region, demonstrating the uniformity of the graphene sample. The G band intensity in the folded region is roughly twice of the intensity collected in the unfolded region because of twice the number of graphene layers in the folded region and out of the resonance range for the twist angle of this sample. As shown in Figure 1f,g, weak D band intensity was collected from the two edges with vertical polarization, while a much stronger D band appears at the horizontal edge in Figure 1g under the horizontal laser polarization. This further confirms that the two edges are armchair and zigzag edges, respectively, and the smooth edge of the exfoliated graphene can be identified as the crystal axis. More information about the edge chirality analysis for the other samples is shown in the Supporting Information (Figures S2 and S3).

2. Observation of the Overtone and Combination Raman Modes in Misoriented Graphene. Figure 2a,b shows respectively the optical and AFM images of a bilayer graphene sheet with six folded regions labeled with 1–6 in Figure 2b. Shown in Figure 2c are the corresponding Raman spectra of the graphene sheet collected in the unfolded region (black line) and folded regions 1–6 in the frequency range of 100–220 cm^{-1} with 632.8 nm laser wavelength. We observe two weak Raman peaks around 115 and 182 cm^{-1} and a stronger one near 123 cm^{-1} in the folded region 6 (red line), and only one peak lying at about 182 cm^{-1} in the regions 3–5, while these modes are not observed in the folded regions 1, 2 and in the unfolded region. Those Raman signals in this range are about 2 orders of magnitude weaker than that of the G band. As discussed below, we assign the peaks at 115 and 123 cm^{-1} to the E_g + ZO′ combination Raman mode and another peak at 182 cm^{-1} to the 2ZO′ overtone mode. As shown in Figure 4a,b, the E_g and ZO′ modes originate from the in-plane shear and out-of-plane breathing modes near the Γ point in the Brillouin zone,[30,41] respectively. The Raman shifts of the combination and overtone modes should equal to the sum of the frequency of the two component phonon modes.[30]

Figure 2d shows the Raman image of the G band intensity of the graphene sheet corresponding to the Figure 2b. The G band signal is obtained over the whole graphene layers, and the intensity in the folded regions is stronger than that obtained in

dx.doi.org/10.1021/jp411573c | J. Phys. Chem. C 2014, 118, 3636–3643

the unfolded region. Figure 2e−g shows the Raman intensity images of the peaks at 115, 123, and 182 cm^{-1}, respectively. The Raman signals centered at 115 and 123 cm^{-1} can only be collected in the folded region 6, and another peak at 182 cm^{-1} can be detected when the laser spot is focused on the folded regions 3−6. Therefore, we consider that the appearance of the new Raman modes is likely to be due to the stacking disorder, and it is closely related to the twist angle between the two graphene layers. What is more, the new Raman modes can only be detected for some special twist angles, while they are invisible for other angles maybe due to the strong spectral background or the dissatisfaction of the resonance condition.[33,53]

Another single layer graphene sample with a folded region is shown in the Supporting Information (Figure S4). A weak Raman peak centered at 850 cm^{-1}, which is an out-of-plane transverse optical phonon mode (oTO), and a relatively strong peak at 121 cm^{-1}, which is assigned to the combination mode E_g + ZO′, appear in the folded region. The G band intensity is surprisingly high (~58 times) in the folded region relative to that measured in the unfolded region, which is due to the fact that the excitation laser energy (E_{laser} = 1.96 eV for 632.8 nm) is close to the energy difference between the valence and conduction of the Van Hove singularities.[10] The twist angle for this graphene sample is about 12°, and this value is defined from the AFM analysis in Figure S6o. This result is also consistent with the critical twist angle where the G band is greatly enhanced.[10] The above experimental results further demonstrate that the new Raman modes recorded in the folded region should be caused by the stacking disorder associated with the folding procedure.

To further analyze the combination and overtone Raman modes, we investigated those Raman modes using different laser excitation energies. Figure 3a−c shows the Raman spectra obtained in the different regions under excitation of 632.8, 532, and 514.5 nm laser lines. Here, we only show the spectra collected in the folded regions 3 and 6 and in the unfolded region. The differences of the feature for these three regions in the frequency range of 50−250 cm^{-1} can be clearly seen in the Raman spectra. Only one Raman mode at 118 cm^{-1} can be observed in the folded region 6, while no any Raman mode appears over the rest of the sample when using 532 nm laser excitation. However, when excited by the 514.5 nm laser line, two Raman modes lying around 113 and 121 cm^{-1} can be observed in the folded region 6, and only one band at 121 cm^{-1} appears in the region 3. The peak at about 95 cm^{-1} near the combination Raman modes in Figure 3a,c is possibly from the IBLM in the twist graphene.[34] Moreover, for the single-layer graphene showing in Figure S4, the dependence of these Raman modes on the excitation laser energy is shown in Figure S5. The Raman mode at 121 cm^{-1} can be observed under 632.8 nm excitation (Figure S5a), while this combination Raman mode cannot be collected when the laser wavelengths are 457.9 and 514.5 nm (Figure S5b,c). These results illustrate that the observation of these new Raman modes are closely related to the incident laser energy. For a given twist angle θ, the Raman mode in the frequency range of 100−200 cm^{-1} can only be observed under specific laser excitation energies and are not observed at other laser excitation energies, which indicates that the origin of these new peaks come from a double resonance process, the same type of process as the D and G′ bands in graphene. We consider that there exists a resonance condition between the twist angle and the laser excitation energy that is necessary for observing the combination and overtone modes in this frequency range. Further work should be carried out to investigate the details of this resonance condition and twist angle dependence in more detail.

In this study, 50 folded graphene samples were investigated. However, only a few of them showed the combination and overtone Raman modes under the excitation laser wavelength that we mentioned before. Figure 3d−f shows the Raman spectra of other samples, from which the combination or overtone Raman modes can be observed. It should be mentioned that, under specific incident laser excitation energies, the combination or overtone Raman modes can be collected on either the twist bilayer (Figure 3d) or a twist few layer graphene sample (Figure 3e) or a disordered stacking sheet with a few-layer graphene on a graphene monolayer (Figure 3f). This further implies that the observation of those new Raman modes should be strongly related to the twist angle between the two graphene layers but independent of the layer number of graphene sheets before being folded.

3. Assignments of the Raman Modes. For the low-frequency phonon modes below 200 cm^{-1}, it is not a hard task to reveal the origin of the observed combination and overtone modes. Here, we assign the two types of low-wavenumber Raman modes as E_g + ZO′ combination and 2ZO′ overtone Raman modes, respectively. The atomic displacements of the two phonon modes are shown in Figure 4a,b. The E_g mode is a

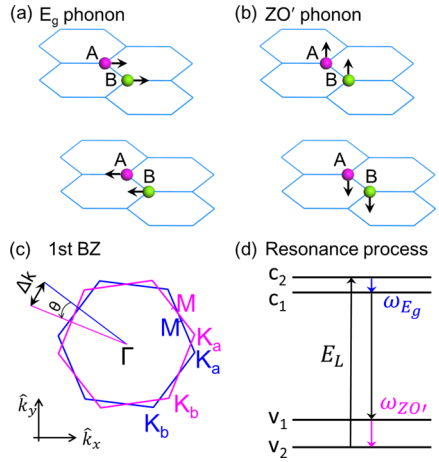

Figure 4. (a, b) Schematic diagrams of the lattice vibrations of the (a) shear mode and (b) ILBM for bilayer graphene at the Γ point of the Brillouin zone. (c) The first Brillouin zone of a misoriented bilayer graphene sample with a twist angle θ between the two layers. (d) A set of a double-resonance processes for the combination Raman mode in misoriented bilayer graphene.

rigid-plane shear mode where the two adjacent layers move to the opposite directions parallel to the layer planes.[39] However, the layer-breathing (ZO′) phonon mode originates from the two carbon atoms in a unit cell of the same graphene layer moving in phase, while the phase of their movements in the adjacent layer are in opposition.[32] These rigid-plane modes in few layer graphene are important because they are directly related to the van der Waals (vdW) interaction between the graphene layers. Considering the phonon dispersion around the Γ point of the Brillouin zone,[32,33] the two phonon modes (E_g and ZO′) can couple with each other as a combination mode, which induces the observation of the modes at about 120 and 180 cm^{-1}. Physically, the coupling of two modes implies that

dx.doi.org/10.1021/jp411573c | J. Phys. Chem. C 2014, 118, 3636−3643

one phonon mode can excite the other phonon mode, which is meaningful in the studies of the phonon modified electric conductance of the bilayer graphene.

Figure 4c shows the structure of two misoriented graphene layers with a twist angle θ between the two graphene layers in reciprocal space. The larger the twist angle, the more separation the two Dirac cones of the two layers are. Stacking disorder between the two layers will form the moiré superlattice structures. The periodic perturbation generated from the moiré pattern will only allow the scattering in which the phonon wave vector ($\mathbf{q}$) matches the reciprocal vectors ($\mathbf{G}$) of the moiré superlattice so that the momentum conservation will be satisfied in the double-resonance Raman process.[24] Figure 4d shows a schematic diagram of the transitions occurring in the double-resonance process for the combination mode, and the overtone mode has a similar process. According to the double-resonance process, there are four virtual transitions that are involved in the Raman scattering processes: (i) the incident photon creates an electron−hole pair ($v_2 \rightarrow c_2$ transition); (ii) the electron is inelastically scattered by a phonon of wave vector $\mathbf{q}$ ($c_2 \rightarrow c_1$); (iii) electron−hole recombination ($c_1 \rightarrow v_1$); (iv) electron−phonon scattering ($v_1 \rightarrow v_2$). When the twist angle is close to the critical value, the scattering between the phonon and electron which are excited by the incident photon is allowed because the momentum conservation is satisfied in this scattering process, and the shear mode and IBLM will be activated so that the combination mode can be detected from the twist graphene samples.

The shear mode and ILBM are two important rigid plane modes in bilayer graphene. In bulk graphite, the corresponding modes are the E^1_{2g} and B^1_{2g} modes,[54] respectively. We consider a linear chain model and assume that interlayer interaction between the adjacent layers is much stronger than that of the nonadjacent layers. Obviously, the restoring force for the rigid plane vibration in bilayer graphene is only present for the interlayer interaction between the two layers, and therefore it is a half of that in graphite, which implies that

$$\omega_{E_g}(\Gamma) = \frac{1}{\sqrt{2}}\omega_{E^1_{2g}}, \quad \omega_{ZO'}(\Gamma) = \frac{1}{\sqrt{2}}\omega_{B^1_{2g}} \tag{1}$$

Since $\omega_{E^1_{2g}}$ and $\omega_{B^1_{2g}}$ at the Γ point in bulk graphite are reported as 42 and 127 cm^{-1}, respectively, the corresponding frequency of ω_{E_g} and $\omega_{ZO'}$ in bilayer graphene are 30 and 90 cm^{-1}.[33,42,55] This estimation for the Raman frequency of the phonon modes is consistent with the frequencies of the shear and breathing modes in few-layer graphene obtained by experimental observation.[30,33]

A theoretical study on the ILBM in a twisted bilayer graphene sample pointed out that the dependence of the ILBM on the twist angle and wave vector is weak,[56] which simplifies our work in assigning the observed new modes. The frequency of the ILBMs will shift (relative to corresponding modes for AB stacked graphene) by less than 10 cm^{-1} when the twist angle is close to the critical value.[34,57] According to double-resonance theory, we determine that the observed peak around 120 cm^{-1} is a combination mode of the shear mode and the ILBM, and the peak around 180 cm^{-1} is the overtone of the ZO′ mode. It is interesting that the combination mode of E_g + ZO′ has a frequency $\omega \approx 120$ cm^{-1}, which is similar to the frequency of the B^1_{2g} mode (∼127 cm^{-1}) in bulk graphite or few-layer graphene. However, this 120 cm^{-1} mode should not be assigned as the B^1_{2g} mode of few-layer graphene, as defined for bilayer graphene sample.

CONCLUSION

In summary, two new Raman modes in the range of 100−200 cm^{-1} are observed in a misoriented few-layer graphene sample with a certain twist angle. The dominant modes in this range are assigned based on the double-resonance Raman process. The Raman mode lying around 120 cm^{-1} is assigned to the combination mode of the rigid in-plane shear mode (E_g) and the ILBM (ZO′) mode. Another mode at ∼180 cm^{-1} is assigned as the overtone mode 2ZO′. The results show that, only for a specific stacking order of graphene layers, will the two Raman modes be greatly enhanced, which allows us to observe them clearly in the Raman spectra. The laser excitation energy dependence of the two Raman modes have been studied in the visible range, suggesting that the second-order Raman modes in this frequency range are closely related to the incident laser energy. Furthermore, the appearance of the Raman modes is independent of the thickness of graphene layers before they are folded. The results demonstrate that stacking disorder will significantly influence these Raman modes and the interlayer interaction in few-layer graphene, which further expands the already powerful ability of Raman spectroscopy to investigate the phonon modes, electron−phonon interaction, and electronic structure in few-layer graphene.

ASSOCIATED CONTENT

Supporting Information

Additional figures for optical image, AFM and Raman spectra. This material is available free of charge via the Internet at http://pubs.acs.org.

AUTHOR INFORMATION

Corresponding Authors

*E-mail: jinzhang@pku.edu.cn (J.Z.).
*E-mail: muwh@itp.ac.cn (W.H.M.).

Notes

The authors declare no competing financial interest.

ACKNOWLEDGMENTS

This work was supported by NSFC (21233001, 21129001, 51272006, and 51121091) and MOST (2011YQ0301240201 and 2011CB932601). M. S. Dresselhaus acknowledges support from NSF (6921903). J. Kong acknowledges support from NSF/DMR-0845358. W. Mu acknowledges support from NSFC (11074259, 11374310), Major Research Plan of NSFC (91027045). Part of theoretical results described in this paper is obtained on the Deepcomp7000 of Supercomputing Center, Computer Network Information Center of Chinese Academy of Sciences.

REFERENCES

(1) Novoselov, K. S.; Geim, A. K.; Morozov, S. V.; Jiang, D.; Zhang, Y.; Dubonos, S. V.; Grigorieva, I. V.; Firsov, A. A. Electric Field Effect in Atomically Thin Carbon Films. *Science* **2004**, *306*, 666−669.

(2) Ling, X.; Xie, L. M.; Fang, Y.; Xu, H.; Zhang, H. L.; Kong, J.; Dresselhaus, M. S.; Zhang, J.; Liu, Z. F. Can Graphene Be Used as a Substrate for Raman Enhancement? *Nano Lett.* **2010**, *10*, 553−561.

(3) Morell, E. S.; Correa, J. D.; Vargas, P.; Pacheco, M.; Barticevic, Z. Flat Bands in Slightly Twisted Bilayer Graphene: Tight-Binding Calculations. *Phys. Rev. B* **2010**, *82*, 121407.

(4) Mu, W. H.; Zhang, G.; Ou-Yang, Z. C. Radius-Voltage Relation of Graphene Bubbles Controlled by Gate Voltage. *Appl. Phys. Lett.* **2013**, *103*, 053112.
(5) Wallace, P. R. The Band Theory of Graphite. *Phys. Rev.* **1947**, *71*, 622−634.
(6) Ni, Z. H.; Wang, H. M.; Kasim, J.; Fan, H. M.; Yu, T.; Wu, Y. H.; Feng, Y. P.; Shen, Z. X. Graphene Thickness Determination Using Reflection and Contrast Spectroscopy. *Nano Lett.* **2007**, *7*, 2758−2763.
(7) Luican, A.; Li, G. H.; Reina, A.; Kong, J.; Nair, R. R.; Novoselov, K. S.; Geim, A. K.; Andrei, E. Y. Single-Layer Behavior and Its Breakdown in Twisted Graphene Layers. *Phys. Rev. Lett.* **2011**, *106*, 126802.
(8) Yan, W.; Liu, M. X.; Dou, R. F.; Meng, L.; Feng, L.; Chu, Z. D.; Zhang, Y. F.; Liu, Z. F.; Nie, J. C.; He, L. Angle-Dependent Van Hove Singularities in a Slightly Twisted Graphene Bilayer. *Phys. Rev. Lett.* **2012**, *109*, 126801.
(9) Havener, R. W.; Zhuang, H. L.; Brown, L.; Hennig, R. G.; Park, J. Angle-Resolved Raman Imaging of Inter Layer Rotations and Interactions in Twisted Bilayer Graphene. *Nano Lett.* **2012**, *12*, 3162−3167.
(10) Kim, K.; Coh, S.; Tan, L. Z.; Regan, W.; Yuk, J. M.; Chatterjee, E.; Crommie, M. F.; Cohen, M. L.; Louie, S. G.; Zettl, A. Raman Spectroscopy Study of Rotated Double-Layer Graphene: Misorientation-Angle Dependence of Electronic Structure. *Phys. Rev. Lett.* **2012**, *108*, 246103.
(11) Carozo, V.; Almeida, C. M.; Ferreira, E. H. M.; Cancado, L. G.; Achete, C. A.; Jorio, A. Raman Signature of Graphene Superlattices. *Nano Lett.* **2011**, *11*, 4527−4534.
(12) Latil, S.; Meunier, V.; Henrard, L. Massless Fermions in Multilayer Graphitic Systems with Misoriented Layers: Ab Initio Calculations and Experimental Fingerprints. *Phys. Rev. B* **2007**, *76*, 201402.
(13) dos Santos, J. M. B. L.; Peres, N. M. R.; Castro, A. H. Graphene Bilayer with a Twist: Electronic Structure. *Phys. Rev. Lett.* **2007**, *99*, 256802.
(14) Tuinstra, F.; Koenig, J. L. Raman Spectrum of Graphite. *J. Chem. Phys.* **1970**, *53*, 1126−1130.
(15) Dresselhaus, M. S.; Dresselhaus, G.; Saito, R.; Jorio, A. Raman Spectroscopy of Carbon Nanotubes. *Phys. Rep.* **2005**, *409*, 47−99.
(16) Nemanich, R. J.; Solin, S. A. 1st-Order and 2nd-Order Raman-Scattering from Finite-Size Crystals of Graphite. *Phys. Rev. B* **1979**, *20*, 392−401.
(17) Malard, L. M.; Pimenta, M. A.; Dresselhaus, G.; Dresselhaus, M. S. Raman Spectroscopy in Graphene. *Phys. Rep.* **2009**, *473*, 51−87.
(18) Xie, L. M.; Wang, H. L.; Jin, C. H.; Wang, X. R.; Jiao, L. Y.; Suenaga, K.; Dai, H. J. Graphene Nanoribbons from Unzipped Carbon Nanotubes: Atomic Structures, Raman Spectroscopy, and Electrical Properties. *J. Am. Chem. Soc.* **2011**, *133*, 10394−10397.
(19) Ferrari, A. C.; Meyer, J. C.; Scardaci, V.; Casiraghi, C.; Lazzeri, M.; Mauri, F.; Piscanec, S.; Jiang, D.; Novoselov, K. S.; Roth, S.; et al. Raman Spectrum of Graphene and Graphene Layers. *Phys. Rev. Lett.* **2006**, *97*, 187401.
(20) Yoon, D.; Moon, H.; Cheong, H.; Choi, J. S.; Choi, J. A.; Park, B. H. Variations in the Raman Spectrum as a Function of the Number of Graphene Layers. *J. Korean Phys. Soc.* **2009**, *55*, 1299−1303.
(21) Ni, Z. H.; Wang, Y. Y.; Yu, T.; You, Y. M.; Shen, Z. X. Reduction of Fermi Velocity in Folded Graphene Observed by Resonance Raman Spectroscopy. *Phys. Rev. B* **2008**, *77*, 235403.
(22) Ni, Z. H.; Liu, L.; Wang, Y. Y.; Zheng, Z.; Li, L. J.; Yu, T.; Shen, Z. X. G-Band Raman Double Resonance in Twisted Bilayer Graphene: Evidence of Band Splitting and Folding. *Phys. Rev. B* **2009**, *80*, 125404.
(23) Sato, K.; Saito, R.; Cong, C. X.; Yu, T.; Dresselhaus, M. S. Zone Folding Effect in Raman G-Band Intensity of Twisted Bilayer Graphene. *Phys. Rev. B* **2012**, *86*, 125414.
(24) Righi, A.; Costa, S. D.; Chacham, H.; Fantini, C.; Venezuela, P.; Magnuson, C.; Colombo, L.; Bacsa, W. S.; Ruoff, R. S.; Pimenta, M. A. Graphene Moire Patterns Observed by Umklapp Double-Resonance Raman Scattering. *Phys. Rev. B* **2011**, *84*, 241409.
(25) Righi, A.; Venezuela, P.; Chacham, H.; Costa, S. D.; Fantini, C.; Ruoff, R. S.; Colombo, L.; Bacsa, W. S.; Pimenta, M. A. Resonance Raman Spectroscopy in Twisted Bilayer Graphene. *Solid State Commun.* **2013**, *175−176*, 13−17.
(26) Zhao, J. L.; Jiang, C. Y.; Fan, Y. W.; Burghard, M.; Basche, T.; Mews, A. Diameter-Dependent Combination Modes in Individual Single-Walled Carbon Nanotubes. *Nano Lett.* **2002**, *2*, 823−826.
(27) Brar, V. W.; Samsonidze, G. G.; Dresselhaus, M. S.; Dresselhaus, G.; Saito, R.; Swan, A. K.; Unlu, M. S.; Goldberg, B. B.; Souza, A. G.; Jorio, A. Second-Order Harmonic and Combination Modes in Graphite, Single-Wall Carbon Nanotube Bundles, and Isolated Single-Wall Carbon Nanotubes. *Phys. Rev. B* **2002**, *66*, 155418.
(28) Cong, C. X.; Yu, T.; Saito, R.; Dresselhaus, G. F.; Dresselhaus, M. S. Second-Order Overtone and Combination Raman Modes of Graphene Layers in the Range of 1690−2150 cm^{-1}. *ACS Nano* **2011**, *5*, 1600−1605.
(29) Mafra, D. L.; Kong, J.; Sato, K.; Saito, R.; Dresselhaus, M. S.; Araujo, P. T. Using Gate-Modulated Raman Scattering and Electron-Phonon Interactions to Probe Single-Layer Graphene: A Different Approach to Assign Phonon Combination Modes. *Phys. Rev. B* **2012**, *86*, 195434.
(30) Lui, C. H.; Malard, L. M.; Kim, S.; Lantz, G.; Laverge, F. E.; Saito, R.; Heinz, T. F. Observation of Layer-Breathing Mode Vibrations in Few-Layer Graphene through Combination Raman Scattering. *Nano Lett.* **2012**, *12*, 5539−5544.
(31) Rao, R.; Podila, R.; Tsuchikawa, R.; Katoch, J.; Tishler, D.; Rao, A. M.; Ishigami, M. Effects of Layer Stacking on the Combination Raman Modes in Graphene. *ACS Nano* **2011**, *5*, 1594−1599.
(32) Sato, K.; Park, J. S.; Saito, R.; Cong, C. X.; Yu, T.; Lui, C. H.; Heinz, T. F.; Dresselhaus, G.; Dresselhaus, M. S. Raman Spectra of Out-of-Plane Phonons in Bilayer Graphene. *Phys. Rev. B* **2011**, *84*, 035419.
(33) Tan, P. H.; Han, W. P.; Zhao, W. J.; Wu, Z. H.; Chang, K.; Wang, H.; Wang, Y. F.; Bonini, N.; Marzari, N.; Pugno, N.; et al. The Shear Mode of Multilayer Graphene. *Nat. Mater.* **2012**, *11*, 294−300.
(34) He, R.; Chung, T.-F.; Delaney, C.; Keiser, C.; Jauregui, L. A.; Shand, P. M.; Chancey, C. C.; Wang, Y.; Bao, J.; Chen, Y. P. Observation of Low Energy Raman Modes in Twisted Bilayer Graphene. *Nano Lett.* **2013**, *13*, 3594−3601.
(35) Popov, V. N.; Henrard, L. Breathinglike Phonon Modes of Multiwalled Carbon Nanotubes. *Phys. Rev. B* **2002**, *65*, 235415.
(36) Podila, R.; Rao, R.; Tsuchikawa, R.; Ishigami, M.; Rao, A. M. Raman Spectroscopy of Folded and Scrolled Graphene. *ACS Nano* **2012**, *6*, 5784−5790.
(37) Spudat, C.; Muller, M.; Houben, L.; Maultzsch, J.; Goss, K.; Thomsen, C.; Schneider, C. M.; Meyer, C. Observation of Breathing-Like Modes in an Individual Multiwalled Carbon Nanotube. *Nano Lett.* **2010**, *10*, 4470−4474.
(38) Lui, C. H.; Heinz, T. F. Measurement of Layer Breathing Mode Vibrations in Few-Layer Graphene. *Phys. Rev. B* **2013**, *87*, 121404.
(39) Saha, S. K.; Waghmare, U. V.; Krishnamurthy, H. R.; Sood, A. K. Phonons in Few-Layer Graphene and Interplanar Interaction: A First-Principles Study. *Phys. Rev. B* **2008**, *78*, 165421.
(40) Jiang, J. W.; Tang, H.; Wang, B. S.; Su, Z. B. Raman and Infrared Properties and Layer Dependence of the Phonon Dispersions in Multilayered Graphene. *Phys. Rev. B* **2008**, *77*, 235421.
(41) Wang, H.; Wang, Y. F.; Cao, X. W.; Feng, M.; Lan, G. X. Vibrational Properties of Graphene and Graphene Layers. *J. Raman Spectrosc.* **2009**, *40*, 1791−1796.
(42) Michel, K. H.; Verberck, B. Theory of Rigid-Plane Phonon Modes in Layered Crystals. *Phys. Rev. B* **2012**, *85*, 094303.
(43) Campos-Delgado, J.; Cancado, L. G.; Achete, C. A.; Jorio, A.; Raskin, J. P. Raman Scattering Study of the Phonon Dispersion in Twisted Bilayer Graphene. *Nano Res.* **2013**, *6*, 269−274.
(44) Wang, Y. Y.; Ni, Z. H.; Liu, L.; Liu, Y. H.; Cong, C. X.; Yu, T.; Wang, X. J.; Shen, D. Z.; Shen, Z. X. Stacking-Dependent Optical Conductivity of Bilayer Graphene. *ACS Nano* **2010**, *4*, 4074−4080.

(45) Poncharal, P.; Ayari, A.; Michel, T.; Sauvajol, J. L. Effect of Rotational Stacking Faults on the Raman Spectra of Folded Graphene. *Phys. Rev. B* **2009**, *79*, 195417.
(46) Poncharal, P.; Ayari, A.; Michel, T.; Sauvajol, J. L. Raman Spectra of Misoriented Bilayer Graphene. *Phys. Rev. B* **2008**, *78*, 113407.
(47) Lu, C. C.; Lin, Y. C.; Liu, Z.; Yeh, C. H.; Suenaga, K.; Chiu, P. W. Twisting Bilayer Graphene Superlattices. *ACS Nano* **2013**, *7*, 2587−2594.
(48) Eckmann, A.; Felten, A.; Mishchenko, A.; Britnell, L.; Krupke, R.; Novoselov, K. S.; Casiraghi, C. Probing the Nature of Defects in Graphene by Raman Spectroscopy. *Nano Lett.* **2012**, *12*, 3925−3930.
(49) Casiraghi, C.; Hartschuh, A.; Qian, H.; Piscanec, S.; Georgi, C.; Fasoli, A.; Novoselov, K. S.; Basko, D. M.; Ferrari, A. C. Raman Spectroscopy of Graphene Edges. *Nano Lett.* **2009**, *9*, 1433−1441.
(50) Krauss, B.; Nemes-Incze, P.; Skakalova, V.; Biro, L. P.; von Klitzing, K.; Smet, J. H. Raman Scattering at Pure Graphene Zigzag Edges. *Nano Lett.* **2010**, *10*, 4544−4548.
(51) You, Y. M.; Ni, Z. H.; Yu, T.; Shen, Z. X. Edge Chirality Determination of Graphene by Raman Spectroscopy. *Appl. Phys. Lett.* **2008**, *93*, 163112.
(52) Cancado, L. G.; Pimenta, M. A.; Neves, B. R. A.; Dantas, M. S. S.; Jorio, A. Influence of the Atomic Structure on the Raman Spectra of Graphite Edges. *Phys. Rev. Lett.* **2004**, *93*, 247401.
(53) Ferrari, A. C.; Basko, D. M. Raman Spectroscopy as a Versatile Tool for Studying the Properties of Graphene. *Nat. Nanotechnol.* **2013**, *8*, 235−246.
(54) Reich, S.; Thomsen, C. Raman Spectroscopy of Graphite. *Philos. Trans. R. Soc. A* **2004**, *362*, 2271−2288.
(55) Dresselhaus, M. S.; Dresselhaus, G.; Saito, R. Physics of Carbon Nanotubes. *Carbon* **1995**, *33*, 883−891.
(56) Cocemasov, A. I.; Nika, D. L.; Balandin, A. A. Phonons in Twisted Bilayer Graphene. *Phys. Rev. B* **2013**, *88*, 035428.
(57) Jiang, J. W.; Wang, B. S.; Rabczuk, T. Acoustic and Breathing Phonon Modes in Bilayer Graphene with Moire Patterns. *Appl. Phys. Lett.* **2012**, *101*, 023113.